Acta Astronautica 154 (2019) 311–319

Contents lists available at ScienceDirect

Acta Astronautica

journal homepage: www.elsevier.com/locate/actaastro

Project Dragonfly: Sail to the stars

Tobias Häfner[a,*,1], Manisha Kushwaha[b,2], Onur Celik[b,3], Filippo Bellizzi[b,4]

[a] Université Paul Sabatier Toulouse, France
[b] Cranfield University, UK

ARTICLE INFO

Keywords:
Interstellar mission
Laser sail
Light sail
Magnetic sail
Alpha Centauri

ABSTRACT

This paper aims to assess the feasibility of an interstellar mission to reach the Alpha Centauri star system and delivering scientific data, using current and near-future technology. The mission baseline uses 100 GW of laser power to accelerate a spacecraft of 2750 kg to 5% the speed of light with light sail technology, resulting in a travel time of about a century. This paper explores several aspects of the mission: Possible locations of the laser infrastructure and different sail materials to achieve the required acceleration are discussed. Deceleration using a magnetic sail in the interstellar medium and in the heliosphere of the target star, taking into account mathematical models from Zubrin [6], Freeman [22] and Gros [21], is studied. Potential orbits in the star system are considered for observation and data collection. Finally, a multi-spacecraft mission architecture is presented, as it would allow for the spacecraft to be launched sequentially, thus exploiting the possibility of continuously operating the laser infrastructure.

1. Introduction

The Alpha Centauri star system is of great interest to the space exploration community, being our closest neighbour and having potential for habitable planets [10,11,12, 23]. It is a binary star system consisting of two stars: Alpha Centauri A and Alpha Centauri B. It is located about 4.3 l y away from the Earth, meaning the furthest travelled manmade objects, the Voyager probes, would take over 70,000 years to reach it.

In 2014, the Initiative for Interstellar Studies (I4IS) announced the Project Dragonfly student competition [34]. The project called for interstellar mission designs, using light-sail based laser propulsion, with the objective of reaching the Alpha Centauri star system within a century. The unmanned interstellar mission should be capable of delivering useful scientific data about the Alpha Centauri star system, associated planetary bodies, solar environment, and the interstellar medium using current or near-future technology.

According to the project brief, a solar powered laser producing a beam of 100 GW is in the vicinity of the earth to propel a light-sail based spacecraft. The travel time to the star system translates into a requirement of an average cruising speed of 5% the speed of light. The project also suggested that decelerating the spacecraft and inserting it into an orbit within the target star system, the time spent at the destination and subsequent information gained would be maximised.

This paper presents a mission design, spacecraft architecture and means for acceleration and deceleration satisfying the description above.

2. Propulsion concepts

Due to the tremendous ΔV required to reach the Alpha Centauri star system within a reasonable time frame, propellant based propulsion systems require a colossal spacecraft [27] to carry the large amounts of fuel. Laser propulsion requires no fuel and as such has an advantage over those systems in terms of mass carried on the spacecraft. In this proposal, a laser system powered by massive solar panels is placed in the vicinity of our sun and, is used to accelerate a light-sail based spacecraft towards the Alpha Centauri star system. Once the spacecraft has arrived at its destination, a magnetic sail creates drag against the interstellar medium and local solar wind [6,21,22], decelerating the spacecraft down to orbital velocities.

* Corresponding author.
E-mail addresses: haefner.tobias@gmail.com (T. Häfner), ahsinam_k@hotmail.com (M. Kushwaha), onur.celik@ac.jaxa.jp (O. Celik), filippomar.bellizzi@gmail.com (F. Bellizzi).
[1] Current: Open Cosmos, UK.
[2] Current: Oxford Space Systems, UK.
[3] Current: The Graduate University for Advanced Studies (SOKENDAI), Japan.
[4] Current: AKKA, Switzerland.

https://doi.org/10.1016/j.actaastro.2018.05.018
Received 28 December 2017; Received in revised form 25 April 2018
Available online 08 May 2018

2.1. Acceleration: laser sailing

2.1.1. Light sail

Light sail has been considered as the primary means of propulsion system for accelerating the spacecraft to attain 5% the speed of light. The idea behind the working principle of the light sail is that the laser system beams photons on to the sail. These photons are then reflected off the highly reflective sail surface, thus propelling the spacecraft by transferring momentum from the laser to the sail.

A spacecraft of total mass m carrying a sail with reflectivity $\tilde{r}$, will accelerate proportionally to the laser power captured by the sail. The acceleration as a function of this power is given by [1].

$$a = \frac{(1+\tilde{r})P}{mc} \tag{1}$$

where c is the speed of light.

As the sail is not perfectly reflective, the absorbed laser energy $(1-\tilde{r})P$ raises the sail with area A and emissivity ε to a temperature of T [1]

$$(1-\tilde{r})P = 2A\varepsilon\tilde{\sigma}T^4 \tag{2}$$

Thus, the thermally limited acceleration is given by [1].

$$\tilde{a} = 2\varepsilon\frac{1+\tilde{r}}{1-\tilde{r}}\frac{\tilde{\sigma}\tilde{T}^4}{\sigma c} \tag{3}$$

Where $\tilde{\sigma}$ is the Stefan-Boltzmann constant, and σ is the total mass per unit area of the sail.

To accelerate the spacecraft, a laser system with aperture diameter D is required to direct the laser beam operating at a wavelength λ onto the sail of diameter d_s at distance s from the laser. The diameter of the sail is given by Refs. [1,4,33],

$$d_s = \frac{2.44\,\lambda s}{D} \tag{4}$$

Where $\frac{2.44\,\lambda}{D} = \theta$ is the diffraction-limited divergence angle of the laser beam. This angle arises from the first null point of the Bessel function for a circular aperture and defines a conde which contains 84% of the laser energy. The remaining laser energy is dispersed outside this cone within the diffraction pattern formed by the aperture [1].

The distance d_{acc} and time t_{acc} at which the spacecraft attains the fraction of speed of light v, without considering the effects of relativistic dynamics, is given by

$$t_{acc} = \frac{v}{a} \tag{5}$$

$$d_{acc} = \frac{vt_{acc}}{2} \tag{6}$$

The acceleration of the spacecraft is dependent on the laser power beamed onto the sail, the areal mass density of the spacecraft (i.e. the overall spacecraft mass per unit area of the sail) and thermal and optical properties of the sail. If the laser power is fixed, the acceleration of the spacecraft can be tuned by using a sail that is highly reflective, has a low density and a high operating temperature. The maximum temperature limit and emissivity of the sail determines the minimum sail diameter for a given laser power, and the sail diameter determines the laser aperture diameter. The aperture diameter is inversely proportional to the sail diameter, i.e. the smaller the sail, the more demanding the laser infrastructure. It is therefore important to identify an optimum ratio of the two parameters.

To obtain a high acceleration, a trade-off was performed between promising sail materials presented in the literature. Their properties are shown in Table 1. It is assumed that the sail accelerates a spacecraft to 5% the speed of light using 100 GW power on the sail, as per the project brief, therefore these two parameters are fixed. The variations in the variables of the sail diameter and corresponding laser aperture diameter are plotted in Fig. 1 using Eq. (7) below (derived from Eq. (1), Eq. (4), Eq. (5) and Eq. (6)), where the total spacecraft mass m is split into spacecraft mass $m_{s/c}$ and sail mass m_s. The spacecraft mass includes 1000 kg payload mass (section 4.4), and 1000 kg magnetic sail mass (section 2.2). The sail mass is further substituted by its density, area and thickness. The third variable of the resulting total time taken to reach the star system is also plotted in Fig. 1. The total travel time includes acceleration, coasting and deceleration.

$$D = \frac{2.44\lambda v^2 c\left(m_{s/c} + \rho\pi t\left(\frac{d_s}{2}\right)^2\right)}{2d_s(1+\tilde{r})P} \tag{7}$$

For a given sail material and diameter, Fig. 1, shows the corresponding laser aperture diameter and the total travel time. It can be seen that the total travel time is not affect much by the choice of the material, however a mono- and multi-layered dielectric sail requires a much larger laser infrastructure compared to the Graphene Monolayer and Graphene Sandwich materials. As a baseline for further calculations, a Graphene Monolayer sail of 29.4 km diameter requiring a 29.4 km laser aperture diameter to reach the Alpha Centauri System within 106.2 years is considered, as a reasonably small sail and laser aperture diameter with acceptable total travel time. The sail area is greater than the minimum required, i.e. 19 km for 100 GW power, as defined by Eq. (2). The mass associated with 29.4 km of sail diameter is 750 kg, hence the total spacecraft mass equals 2750 kg after accounting for the payload and magnetic sail. The resulting acceleration for this spacecraft mass and laser combination is 0.127 m/s^2 (Eq. (1)). The time required to accelerate to 5% of speed of light is 3.7 years (Eq. (5)) and distance at which the speed is attained is 5909AU (Eq. (6)).

2.1.2. Laser system

A good location is essential to use the laser infrastructure efficiently and safely. For a trade-off, the following requirements have been used: 1) The target, Alpha Centauri, shall be visible and never be eclipsed by a nearby celestial body. 2) The laser shall never be under any solar eclipse. 3) The solar irradiation level shall be at least as high as on Earth. 4) It shall be reachable for human spaceflight, for assembly and maintenance purposes. 5) It shall be impossible to focus the laser beam

Table 1
Sail materials.

Material	Max. Temp (K)	Density (gr/cm^3)	Reflectivity (%)	Absorptivity (%)	Emissivity (%)	Thickness (nm)	Wavelength (nm)
Graphense Based							
Graphene Monolayer [5,31],	450	2.21	5	40	3	0.5	Not studied
Graphene Sandwich [5,29,31],	4500	10	5	3	3	0.335	Not Studied
Dielectric							
Alumina (Al203) [2]	2327	3.96	26	84	90	57	400
Silicon Carbide [3,4]	2000	3.17	56	44	85	38	400
Multi-Layered Dielectric							
Ag, SiO2, TiO2 5-layers [29]	1235	1.4	99.61	< 0.39	3	1000	1060
Ag, SiO2, TiO2 15-layers [29]	1235	1.4	99.995	< 0.005	3	1000	1060
Cu, SiO2, TiO2 15-layers [29]	1360	1.4	99.993	< 0.003	7	1000	1060

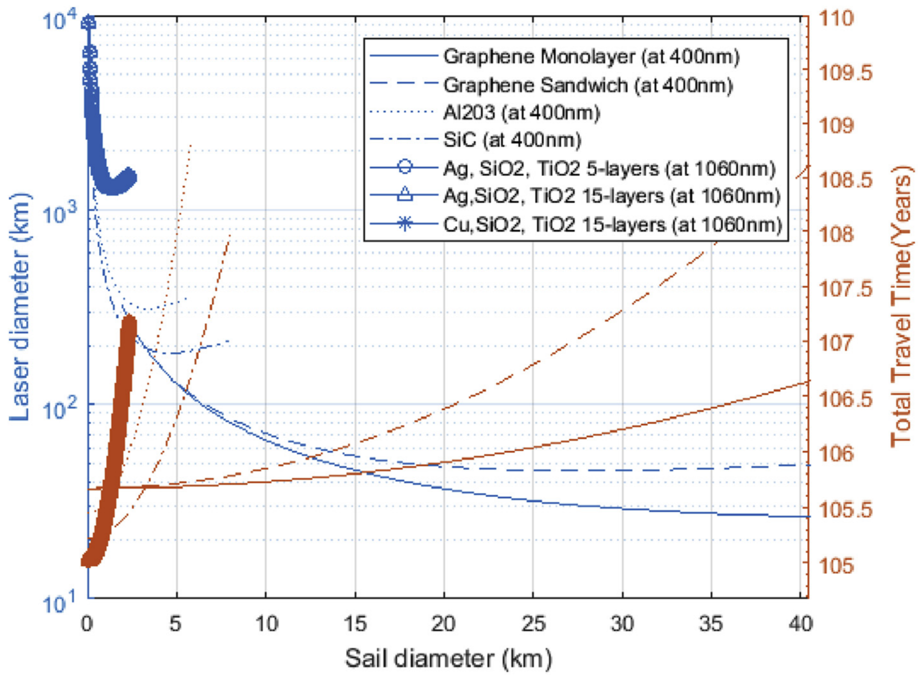

Fig. 1. Sail diameter vs laser diameter and total travel time.

onto the Earth's surface. 6) To reach a long operation time, the orbit must be stable (little fuel consumption) and must be free of space debris.

Several locations have been analysed and summed up hereafter: 1) Antarctica: Would be easy to reach and the target is always visible. Its problems are long solar eclipse periods and pointing errors due to atmospheric disturbances. 2) LEO: Both sun and the target will often be hidden by the Earth. Additionally, busy orbits with a lot of debris make it not suitable for a big structure. 3) Cislunar: Sun and target will always be visible. At the same time, the laser would be relatively close to Earth, so that the Earth's surface would not be in the focal range of the system. Also, it is relatively free of orbital debris, but still accessible from Earth for construction and maintenance. It becomes even more interesting if synergies with lunar exploration could be used. 4) Lagrange Point 3 (L3), 1AU behind the sun, would be very safe, as pointing towards Earth is not possible. On the other hand, L3 would be very difficult to reach the laser for assembly and maintenance. 5) Lagrange Point 1 (L1), between the Earth and the sun, is favourable for harvesting solar power due to high irradiation. However, the laser would be difficult to reach for assembly and maintenance. 6) Lunar surface might be interesting from a construction point of view, as Perakis et al. [30] highlight. Whether a location with constant solar irradiation and constant visibility of the target exists would need to be investigated.

Overall, L1 and a cislunar orbit seem favourable, L1 offering extra solar power, and cislunar orbit good accessibility.

100 GW of laser power is needed on the spacecraft sail to propel it to high velocities. As the spacecraft travels a large distance during the acceleration phase, the laser optics must be able to adjust their focus accordingly. Without such a feature, most of the power would be lost into space, drastically decreasing the efficiency of the system and making high end velocities unfeasible. The minimal distance where the laser propulsion comes into play is assumed to be 2 AU, but depends on the initial transfer orbit strategy. Because Alpha Centauri is located off-plane with reference to our planetary disk, it might be difficult to create a useful thrust vector with the laser from the beginning. Instead, the spacecraft would presumably perform some planetary swing-by manoeuvres to gain its initial speed and reach a flight direction towards Alpha Centauri. As calculated in section 2.1.1, the acceleration phase takes 3.9 years, in which the spacecraft travels $8.840{\cdot}10^{11}$ km (5909AU). The laser focus must therefore be adjustable between 2 AU and 5909 AU. For safety reasons and as stated in location requirement 5, it is important that the Earth is not within the focal range of the laser. It is therefore important that the laser cannot focus onto a target closer than the range needed. Assuming the minimal focus distance f of 2 AU ($3{\cdot}10^8$ km), a cislunar orbit of 300,000 km altitude, a laser lens diameter d of 29.4 km (section 2.1.1), and 100 GW of power P, the maximum possible power density on Earth surface is 148 W/m^2 according to Eq. (8) and therefore not harmful.

$$pd = \frac{P}{\left(\frac{f-a}{f}\frac{d}{2}\right)^2 \pi} \tag{8}$$

The laser's pointing accuracy must be high enough to point towards the spacecraft at a distance of $8.840{\cdot}10^{11}$ km. If an acceptable offset of 1000 m at the sail is assumed, that corresponds to a pointing accuracy of $6.5{\cdot}10^{-11}$ degrees. Achieving this will be challenging from an actuation and controlling point of view (as a comparison, James Webb absolute pointing accuracy is expected to be $> 10^{-6}$ degrees [28]). Also, the time delay in a pointing control loop involving feedback from the spacecraft would be more than two months due to roundtrip travel time of light and information.

As described with Eq. (4), focussing a laser accurately becomes less critical as the wavelength becomes smaller and the lens diameter of the laser system scales directly with it. Therefore, the wavelength of the laser should be chosen as small as technically achievable. A wavelength of 400 nm has been chosen for this study as a reasonable assumption and in accordance with wavelengths used to characterise sail materials, as described in section 2.1.1.

2.2. Deceleration: magnetic sail

Different concepts for decelerating the spacecraft after an interstellar travel can be found in the literature. The most prominent are magnetic sail [6,21,22], electric sail [26], combinations of both [25], and photonic sails (as presented in this paper for acceleration purposes). For deceleration, a photonic sail has been discarded in order to avoid dependence on any laser infrastructure towards the end of the mission. Relying exclusively on sun light for deceleration as described by Heller and Hippke [32] appears not to be suitable for a spacecraft of the studied size due to the high forces and temperatures related to the concept. Instead, a way to use a magnetic sail as an interstellar break as well as a mean to manoeuvre within the target star system is presented. The concept does not require an additional electric sail to enhance performance.

The concept is outlined using magnetic sail and interstellar medium properties from Zubrin and Martin [6]. At the end of the section, alternative magnetic sail models from Gros [21] and Freeman [22] are also considered. The impact of uncertainties about interstellar medium properties, as estimated by Crawford [24], is also discussed.

Zubrin and Martin [6] derive the force generated by a magnetic sail using a particle – magnetosphere interaction model. The resulting force F is given by Eq. (9), where ρ is the plasma density, μ is the permeability of free space, I is the current in the magnetic sail loop, R is the loop radius and υ is the velocity.

$$F = 1.175\pi\left(\rho\mu^{\frac{1}{2}}IR^{2}\upsilon^{2}\right)^{\frac{2}{3}} \tag{9}$$

The force and corresponding acceleration are functions of the velocity. A differential equation can be formed and solved, giving the expression for the velocity as Eq. (10) and Eq. (11)

$$\upsilon(t) = \frac{\upsilon_0}{\left(1 + \frac{const}{3}\upsilon_0^{\frac{1}{3}}t\right)^{3}} \tag{10}$$

$$const = \frac{1.175}{m_{s/c}}\pi\left(\rho\mu^{\frac{1}{2}}IR^{2}\right)^{\frac{2}{3}} \tag{11}$$

The deceleration phase of the spacecraft would take place in two different environments: It begins in the interstellar space and will be completed within the heliosphere of the Alpha Centauri system. For calculations, it is assumed that the interstellar space has a plasma density of $1.67{\cdot}10^{-22}$ kg/m^3 [6], and this plasma has no significant bulk velocity.

The properties of the heliosphere, used in Eq. (12) and Eq. (13), are the values from our solar system and have a limited validity for Alpha Centauri. They are used here on the basis that Alpha Centauri A and B show comparable mass and luminosity properties as our sun and shall give us an idea of the expected environment. The solar wind of the star has been assumed to have a constant velocity of $5{\cdot}10^5$ m/s. Its density is dependent on the distance from the star and follows Eq. (12) [6], where R is the distance to the star in astronomical units.

$$\rho\left[\frac{kg}{m^3}\right] = \frac{8.35.10^{-21}}{R^2} \tag{12}$$

The heliopause, where the solar wind is suddenly stopped by the interstellar medium, is at a distance of 120 AU or $1.8{\cdot}10^{13}$ m from the star. The gravitational pull from the star is negligible for this calculation and follows Eq. (13), resulting in 0.0059 m/s^2 at 1 AU, or $4{\cdot}10^{-7}$ m/s^2 at 120 AU (using the sun's properties). As depicted in Fig. 2, this is several orders of magnitude below the deceleration produced by the magnetic sail.

$$g = G\left(\frac{M}{r^2}\right) \tag{13}$$

The following design parameters lead to a reasonable deceleration profile: A magnetic sail mass of 1000 kg, assuming a wire density of 9000 kg/m^3 and a wire cross section of 1 mm^2, forming a loop of 35,368 m diameter. The total spacecraft mass at that time will be 2000 kg, as the light sail has been jettisoned after the acceleration phase. According to this model, a current density of $1.52{\cdot}10^{11}$ A/m^2 would be required. Current densities in the order of 10^{11} A/m^2 have already been achieved at least in lab conditions [7]. Nevertheless, fabricating a sufficiently strong and thin wire out of such a superconductor will be challenging. By applying the parameters and initial coasting velocity of 5% the speed of light to Eq. (10), a deceleration profile as seen in Fig. 2 is generated. The deceleration takes place over 20.8 years and over a distance of 7500 AU ($1.12{\cdot}10^{12}$ km).

An important part of the deceleration happens in the end of the deceleration process, when the spacecraft is under the influence of the solar wind. As the produced force decreases with decreasing velocity, the magnetic sail becomes ineffective at low speeds in interstellar space. However, after entering the heliosphere, this changes. Fig. 3 show this final stage. The spacecraft crosses heliopause 20 years after the start of the deceleration. As the plasma density behind the heliopause is lower than in interstellar space, there is nearly no breaking effect in the outer heliosphere. But further inside, with increasing density and the additional velocity of the solar wind, the deceleration reaches a maximum. As the velocity further decreases, deceleration decreases again. The simulation plot ends at a distance of 1AU from the target star with a velocity of 250,400 m/s. From this location on, the magnetic sail can be used to navigate to any orbit. By changing the attitude of the sail with respect to the solar wind, any force vector needed to change orbital parameters can be generated [6].

A magnetic sail needs to provide sufficient performance margin to account for two main uncertainties: The exact parameters of the local

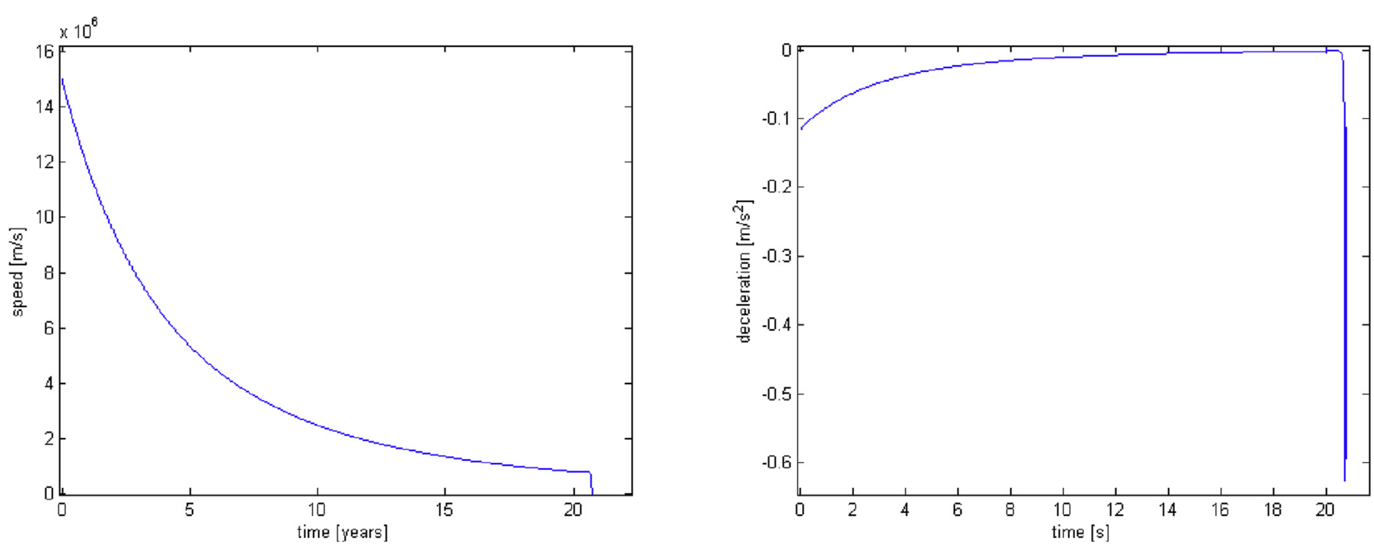

Fig. 2. Deceleration using a magnetic sail: Velocity and deceleration profile.

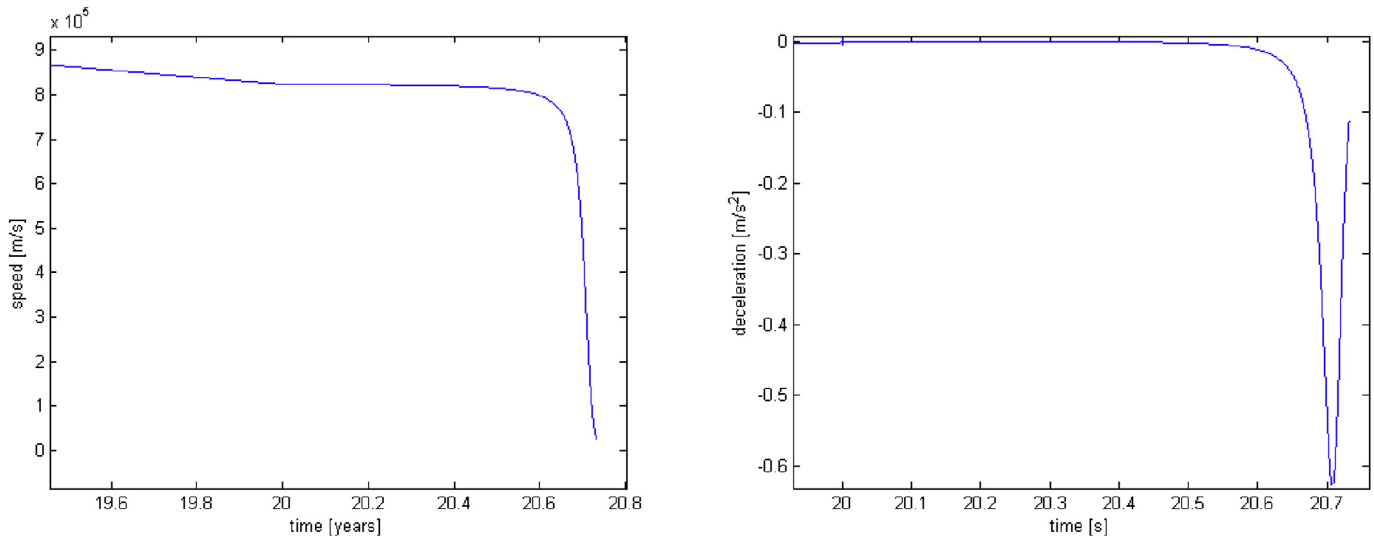

Fig. 3. Deceleration using a magnetic sail within the heliosphere: Velocity and deceleration profile.

environment, and the real interaction mechanism with it.

New models of the interaction of a magnetic sail with its environment have been published since the Zubrin and Martins paper, namely Gros [21] and Freeman [22]. They both come to a more pessimistic conclusion concerning deceleration performance. Freeman refined Zubrins model and gives the decelerating force as in Eq. (14).

$$F \approx 0.354\pi\,(\mu_0 I^2 a^4 \delta^2 v^4)^{\frac{1}{3}} \tag{14}$$

Gros based the model on numerical simulations, which leads to a different type of deceleration profile. It is governed by Eq. (15) and Eq. (16), where I_C is the critical current, estimated to be $1.55{\cdot}10^6 A$.

$$x_{max} = \frac{1/0.081}{\log^2\left(\frac{v_0 I_c}{cI}\right)} \frac{1}{4m_p n_p} \frac{m_{tot}}{\pi R^2} \tag{15}$$

$$v = v_0 e^a \exp\left(\frac{-a}{\sqrt{1-\frac{x}{x_{max}}}}\right), \quad \text{where } a = \log\left(\frac{cI}{v_0 I_C}\right) \tag{16}$$

There are several possibilities to adjust the performance of a magnetic sail. Increasing the loop diameter as well as increasing the wire cross section is straight forward but ineffective as it also increases the mass to be decelerated. This approach therefore leads to prohibitive sail masses which can reach up to 10^3 metric tonnes for a comparable sample mission [21]. The more promising approach from a systems perspective is to increase the current density in the superconductor.

Estimations of the hydrogen density between our and the Alpha Centauri solar systems vary between 0.15 and 0.43 particles/cm^3, with an ionisation fraction between 0.17 and 0.5 [24]. That translates into an uncertainty of ionised mass density of one order of magnitude ($4.23{\cdot}10^{-23}$ kg/m^3 to $3.57{\cdot}10^{-22}$ kg/m^3).

Taking the worst-case hydrogen density and the mission baseline of this paper into account, Zubrins model requires a current density of $6{\cdot}10^{11}$ A/m^2 to achieve the targeted performance, Freemans model $3.6{\cdot}10^{12}$ A/m^2 and Gros model $4.8{\cdot}10^{14}$ A/m^2. Fig. 4 depicts a comparison between the resulting deceleration profiles.

Freeman [22] shows how the achievable current density in superconductors increased over the past years and is approaching $10^{11} A/m^2$. Although the necessary values, especially according to Gros model, are not feasible yet, they might become reachable in the next decades.

3. Mission baseline scenario

Our understanding about what lies beyond the solar system is limited to Earth-based telescope observations and few in-situ data provided by spacecraft that passed heliopause. There are still numerous unknowns about the interstellar medium and other star systems, therefore any data transmitted back to Earth will be very important to enhance our knowledge. A flyby mission through the target star system would be a minimum risk alternative, but less data would be gathered. In this direction, the mission baseline is created to obtain the maximum scientific return out of this ambitious mission.

The mission is broken down into four targets that will be investigated specifically. Those are:

(1) Mutual interaction of Alpha Centauri A and B
(2) Understanding Alpha Centauri A
(3) Understanding Alpha Centauri B
(4) Understanding Proxima Centauri-Planet system

These targets are listed without considering a preference or a priority between them. However, it seems clear that a precursor mission to map the system and understand the overall properties of Alpha Centauri system would be useful. In addition to that, the observation of a newly discovered planet around Proxima Centauri [8] would also be one of the primary goals. In fact, Proxima Centauri is closer to our solar system compared to Alpha Centauri A and B. The planet around Proxima Centauri, when visited, will most likely be the first ever exoplanet visited.

A single spacecraft mission would be very restrictive to fulfil these exploration goals. Even to visit two different targets, a demanding mission optimization would likely be inevitable. A "single spacecraft, multi-objective" type mission appears to be likely only for first three targets outlined above, as Proxima Centauri and its companion planet is about 13,000 AU or 0.21 ly away from the binary star system [9]. To achieve all four targets, a multi-spacecraft scenario with four identical large-class spacecrafts will be employed, each targeting one aspect of the star system as listed above. An illustration of the mission baseline scenario can be seen Fig. 5.

It is foreseen that the laser system can propel one spacecraft at a time. Therefore, the spacecrafts will be launched with a 3.7 years' time difference between them. Note that this is the time required to accelerate one spacecraft to 0.05c. Thus, the laser system will be in almost continuous operation for ~15 years, except during transition times between two successor spacecrafts.

As spacecraft will be launched one after the other, it is possible to prioritize the mission targets. It seems, as discussed earlier, that (1) and (4) are more desirable in terms of getting to know the basic properties

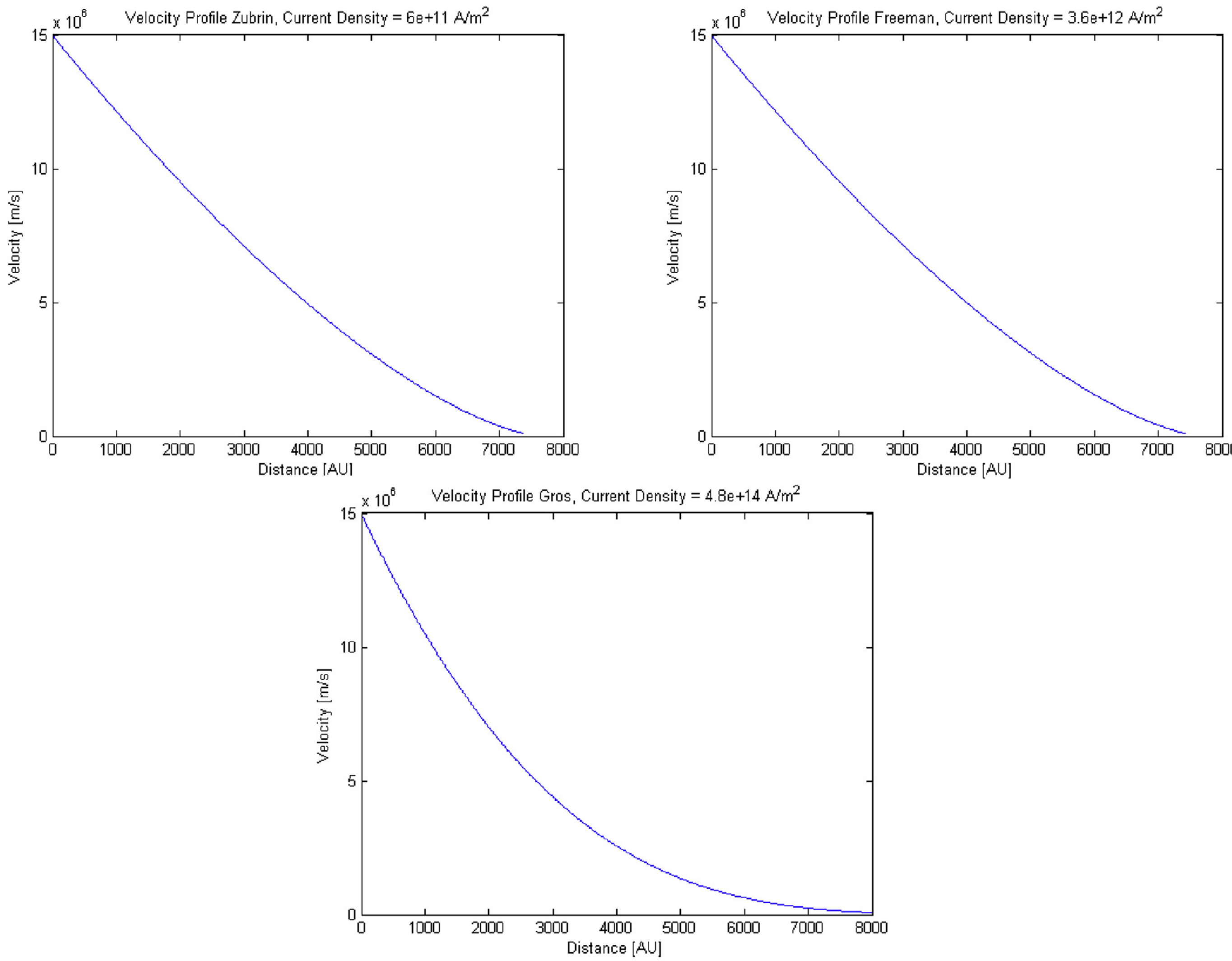

Fig. 4. Deceleration profiles using different magnetic sail interaction models.

of the star system and visiting the closest exoplanet. The first launched spacecraft can be Dragonfly-(1), referring to its target with the number in the parenthesis, whereas the second would be Dragonfly-(4), as they will reach at approximately the same time, as Proxima is closer to the solar system. The third and fourth launch would be interchangeable based on scientific interest.

It is worth noting that a rapid development in the laser technology could allow a spacecraft to propel higher than 0.05c after initial launch. Allowing the successor spacecraft to overtake the previous one. This case is not considered in this study.

3.1. Mission phases

The mission is mainly broken down into three phases: acceleration, cruise and deceleration. There are phases preceding and succeeding those, namely the transfer to the acceleration point and the operational

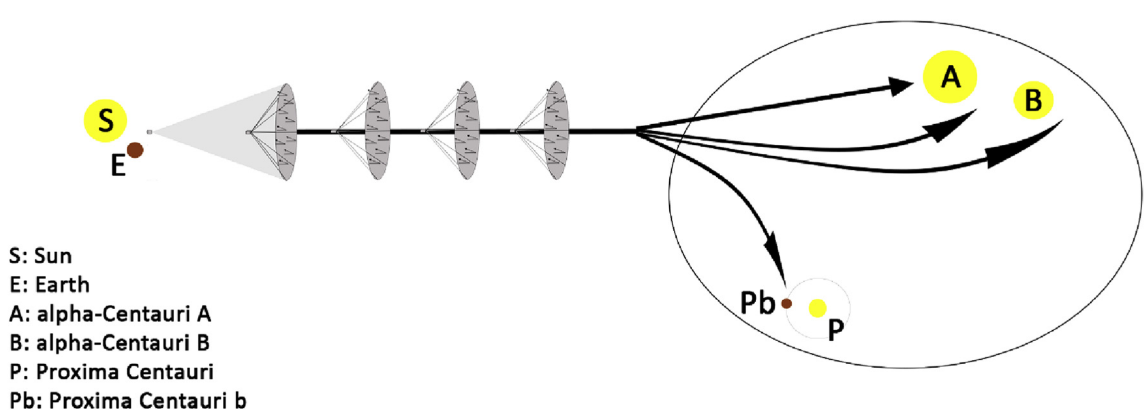

Fig. 5. Illustration of Dragonfly mission baseline scenario.

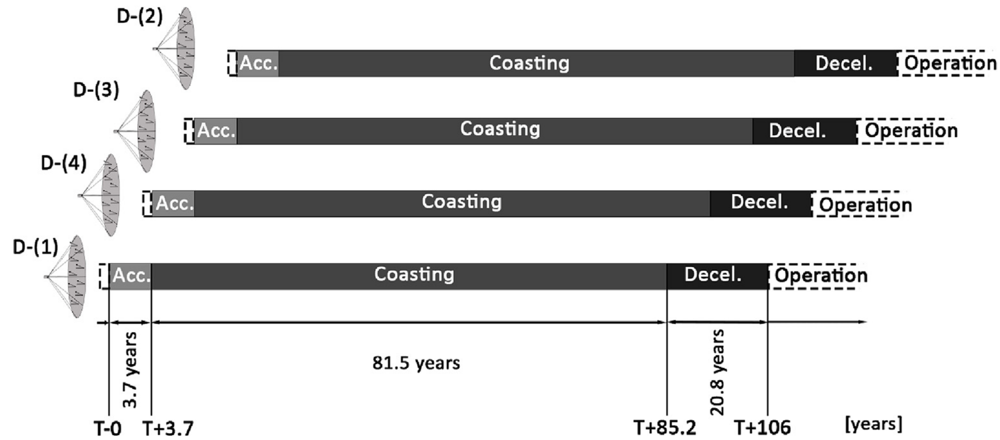

Fig. 6. Illustration of Dragonfly mission timeline.

phase at Alpha Centauri respectively. Since the transfer time is very small compared to the ~100-year mission timeframe, it is not discussed here. This section provides the mission timeline for one Dragonfly spacecraft weighing 2750 kg at launch. The other spacecraft follow the same timeline.

Acceleration: The acceleration phase starts at T-0 and the spacecraft is accelerated to 0.05c in 3.7 years. It will reach 5909 AU (0.09 l y) at the end of this phase. Once the acceleration phase finishes, the light sail will be jettisoned from the spacecraft to decrease the weight of the spacecraft, reduce damages due to micrometeoroid environment and avoid attitude control problems due to sail rip-off.

Coasting: The cruise phase begins right after the acceleration phase at T + 3.7 years. The spacecraft will cruise at 0.05c for 81.5 years up till 4.18 l y (7500 AU away from Alpha Centauri). When this phase starts, the laser would briefly cease operation until the next Dragonfly spacecraft transfers to its acceleration point.

Deceleration: The phase takes the last 20.8 years of the voyage, starting at T + 85.2 years. The deceleration will be performed by the magnetic sail, as explained in section 2.2, and will continue until the spacecraft decelerates to near orbital speeds at T + 106 years.

The timeline of the mission is provided in Fig. 6, without indicating a launch date.

3.2. *Operational phase at Alpha Centauri*

The duration of the operational phase is still uncertain. However, it can be assumed that the spacecraft shall be operational when the first data is exchanged. The total duration of the mission then becomes minimum of ~8.6 years (data travel time is approximately 4.3 years one-way). Therefore, the mission is assumed to last at least 10 years for each spacecraft, plus another ~4.3 years of receiving data back on Earth.

In order to enhance the scientific return, two orbit options are evaluated for the Dragonfly spacecraft. Halo orbits around Lagrange points are widely used for astronomy and solar observation missions, as they provide continuous observation of stars. As considered for the Dragonfly laser system, a halo orbit could be a good fit for understanding the mutual interaction of Alpha Centauri A and B. Dragonfly-(1) could be placed at the Centauri A-B L1 point, between the two bodies, where it can observe both stars continuously and measure the interaction of both stellar winds. While these assets make L1 point an interesting location for science, its characteristics need to be carefully examined. As opposed to well understood Lagrange points in our solar system, the mutual orbit of Alpha Centauri A and B is highly elliptic with a very large semi-major axis of 11.2 AU (approximately Sun-Saturn distance) [19]. Therefore, station-keeping might be a challenge.

The second alternative could be Quasi-Satellite Orbits (QSO), which are also known as Distant Retrograde Orbits (DROs) in the literature. QSOs were also considered for Martian moons missions, as well as asteroid retrieval missions. They are usual Keplerian orbits in formation with a smaller planetary body in a three-body system, therefore always in the vicinity of it. Such orbits can be utilized to observe Proxima b, without being too close to Proxima Centauri, as the planet-star distance is only 0.05 AU [20]. QSOs are known to be stable for long durations, thus could be a less risky alternative, while increasing observation opportunities.

4. Spacecraft architecture

The following section gives a brief overview over some features and peculiarities concerning spacecraft architecture for the Dragonfly mission.

4.1. *Payload*

Two recent exploration missions in our own solar system are used as a reference for payloads which study a star and the planetary bodies around it.

To study a star and its heliosphere, NASAs Advanced Composition Explorer (ACE) mission has a good example of instruments that might be useful [13]. ACE studies the energetic particles from the solar wind, the interplanetary medium, and other sources. The set of 8 instruments can be used to perform similar studies at Alpha Centauri star system. They sum up to a mass of 128.5 kg and 136 W of power consumption.

To estimate the mass needed to study planets around Alpha Centauri, the Cassini mission is used as a reference [14]. This set of instruments has been used to study the solid surface of Titan, the gaseous Saturn as well as its rocky rings. It therefore seems well suited to study planets with yet little-known characteristics. These instruments sum up to a mass of 269 kg and a power consumption 382 W.

As seen in the mass budget in section 4.4 and power estimation in section 4.2, it is not possible to accommodate all these instruments in one single spacecraft travelling to Alpha Centauri. Making use of the multi-spacecraft mission architecture, they need to be distributed over three spacecrafts.

4.2. *Power subsystem*

During this long travel, the spacecraft will need a fair amount of power to collect data through sensors but also to keep all its systems working. Because of the distance from every light source, solar panels are not an option. As for most deep space probes, the most suitable power source will be nuclear RTGs. The RTG (radioisotope thermoelectric generator) technology is based on the production of electric

Table 2
Mass Budget for one spacecraft.

Payload	135 kg
Power System	165 kg
AOCS/GNC	200 kg
Structure and thermal	300 kg
Communication	200 kg
Light sail	750 kg
Magnetic sail	1000 kg
Total	2750 kg

power from the radiative decay of an isotope (Plutonium, Americiu, Pb-Te, etc.).

The power consumption of the spacecraft is estimated to be around 300 W. This considers a 180 W payload, 100 W communication system, AOCS, computation and thermal systems, and the fact that these systems will never operate at full power simultaneously. The efficiency of RTGs drops over time, mainly due to deterioration of the used thermocouples [15]. At the end of the mission, after one hundred years of travel, the efficiency is estimated to be 45%. Considering an RTG type with high power density (5 W/kg for GPHS-RTG) [15] and 25% overhead mass, the power subsystem will have a mass of around 165 kg.

4.3. AOCS/GNC subsystem

In terms of AOCS, a similar proposal by Drai [16] for a heliopause bound probe based on solar sail technology is used as a reference. It is estimated that the AOCS equipment mass will be 7% of the total spacecraft mass, which is 200 kg.

Determining the position of a spacecraft in space is currently done by working out the difference in time that radio communications take to travel to and from a probe. By entering deeper into interstellar space these algorithms become less accurate, having an error rate of 4–10km/AU [17]. To overcome this problem, Becker [18] explains how the regular light signals from Pulsars can be used to determine the position of a spacecraft. The system is based on comparisons between pulse arrival times at the spacecraft with pulse arrival times at a reference location.

4.4. Mass budget

As seen in section 2.1.1, the initial overall mass of the spacecraft cannot exceed 2.75 metric tons in order to achieve the required acceleration. Considering all the mass estimations, the following mass budget is established, whereas the masses for structure and communication are estimated generically (see Table 2).

A spacecraft of nearly 3 metric tonnes might appear odd compared to the current trend of miniaturisation in the space community down to chip sized spacecraft. Recent research for Breakthrough Starshot [29] shows that spacecraft bus and light sail are scalable. In this case the laser power can be substantially reduced as presented by Lubin [29].

The magnetic sail for deceleration is a main mass driver. As Eq. (11) shows, the total spacecraft mass, the magnetic sail diameter and the current in it need to be balanced for a given performance. When fixing the mass ratio between sail and spacecraft body, the required current depends on the spacecraft mass only. Using Zubrin and Freemans models, the required current scales according to Eq. (17).

$$I \sim \frac{1}{\sqrt{m_{SC}}} \tag{17}$$

Using Gros model, the scaling is more complex, but a few numerical simulations show that the relation is even worse. Considerably downsizing an interstellar orbiter which relies on magnetic sail for deceleration appears not to be feasible due to the current density limitations in a superconductor.

5. Conclusion

A mission design to send standard sized spacecrafts to Alpha Centauri star system, using current or near-future technology, was presented. Laser sails can accelerate several tons of mass to 5% of speed of light, leading to a transfer time of around a century. Magnetic sails are suitable to decelerate from such velocities, especially when making use of solar wind at the target solar system. Both technologies have the benefit that no propellant needs to be transported in the spacecraft. As a drawback, they require kilometer-sized structures in space. With a multi-spacecraft mission baseline, the laser system is used over a reasonable period of time. Lessons learned and data gathered from the first spacecraft could be used to enhance the following ones.

The mission is based on technologies that are currently available or under development, but would need extensive improvements to actually build the required space infrastructure. In-orbit fabrication and assembly are crucial to build the required structures. Materials for the light sail and the magnetic sail need to reach the required characteristics and technical readiness level. Further challenges include the high power laser system, its pointing control and accuracy, communication over such distances, and the lifetime of all systems.

Acknowledgments

Special thank from the team goes to the organising committee which includes Andreas Hein and the I4IS organisation for the opportunity and BIS for hosting the presentation. We would also like to acknowledge other members of the team, namely Andrea Testore, Chengyu Ma, Chiara Palla, Divya Shankar, George Muntean, Kieran Hayward, Mahbub Rahman, and Thomas Andreu.

References

[1] Colin R. McInnes, Solar Sailing: Technology, Dynamics and Mission Applications, (2013).
[2] G. Landis, Advanced Solar and Laser Pushed Lightsail Concepts, (1999).
[3] G. Landis, Optics and materials considerations for a laser-propelled lightsail, Paper IAA (1989) 89–664 40th IAF Congress, Torremolinos Spain, October.
[4] G. Landis, Small laser-propelled interstellar Probe, Paper IAA-95-IAA.4.1.102, 46th IAF Congress, Oslo Norway, October, 1995.
[5] G.L..Matloff, Graphene:The ultimate interstellar solar sail material, J. Br. Interplanet. Soc. (JBIS) 65.pp.378-384.
[6] Robert Zubrin, et al., The Magnetic Sail - Final Report to the NASA Institute of Advanced Concepts, (2000) January 2000.
[7] L. Fang, et al., Huge critical current density and tailored superconducting anisotropy in SmFeAsO0.8F0.15 by low-density columnar-defect incorporation, Nat. Commun. (2013) 2655.
[8] G. Anglada-Escudé, et al., A terrestrial planet candidate in a temperate orbit around Proxima Centauri, Nature 536 (7617) (2016) 437–440.
[9] P. Kervella, F. Thévenin, C. Lovis, Proxima's orbit around α Centauri, Astron. Astrophys. 598 (2017) L7.
[10] A. Bixel, D. Apai, Probabilistic constraints on the mass and composition of Proxima b, Astrophys. J. Lett. 836 (2017) L31.
[11] X. Dumusque, F. Pepe, C. Lovis, D. Ségransan, J. Sahlmann, W. Benz, F. Bouchy, M. Mayor, et al., An Earth mass planet orbiting Alpha Centauri B, Nature 490 (7423) (2012) 207–211.
[12] Vinesh Rajpaul, Suzanne Aigrain, Stephen J. Roberts, Ghost in the time series: no planet for Alpha Cen B, Mon. Not. Roy. Astron. Soc. 456 (2015) L6.
[13] https://directory.eoportal.org/web/eoportal/satellite-missions/content/-/article/ace#sensors.
[14] http://sci.esa.int/cassini-huygens/.
[15] Lee S. Mason, Realistic Specific Power Expectations For Advanced Radioisotope Power System, NASA John H. Glenn Research Center at Lewis Field, Cleveland, Ohio 44135.
[16] Remi Drai, Bogdan Udrea, Stephanie J. Thomas, Integrated attitude and orbit control of an interstellar heliopause probe, Aerospace Conference, 2007 IEEE, IEEE, 2007.
[17] Jonathan Amos, Dead Stars, to guide spacecraft, Manchester, 2012http://www.bbc.co.uk/news/science-environment-17557581.
[18] Werner Becker, How interstellar beacons could help future astronauts find their way across the universe, Royal Astronomical Society, 2012. http://www.ras.org.uk/news-and-press/219-news-2012/2111-how-interstellar-beacons-could-help-future-astronauts-find-their-way-across-the-universe, .
[19] W. Hartkopf, D.M. Mason, Sixth catalog of Orbits of visual binaries, U.S. Naval Observatory, 2008.

[20] Ignasi Ribas, Emeline Bolmont, Franck Selsis, et al., The Habitability of Proxima Centauri B: I. Irradiation, Rotation and Volatile Inventory from Formation to the Present, (25 August 2016) arXiv:1608.06813.
[21] Claudius Gros, Universal scaling relation for magnetic sails: momentum braking in the limit of dilute interstellar media, J. Phys. Commun. (2017).
[22] M. Robert, I.I. Freeland, Mathematics of Magsails, J. Br. Interplanet. Soc. (JBIS) 68 (2015) 306–323.
[23] G. Anglada-Escudé, P.J. Amado, J. Barnes, Z.M. Berdiñas, R.P. Butler, G.A. Coleman, ... S.V. Jeffers, A terrestrial planet candidate in a temperate orbit around Proxima Centauri, Nature 536 (7617) (2016) 437–440, http://dx.doi.org/10.1088/2399-6528/aa927e.
[24] I. Crawford, Project Icarus: a review of local interstellar medium properties of relevance for space missions to the nearest stars, Acta Astronaut. (2011).
[25] Nikolaos Perakis, Andreas M. Hein, Combining magnetic and electric sails for interstellar deceleration, Acta Astronaut. (2016).
[26] P. Janhunen, Electric sail for spacecraft propulsion, J. Propulsion Power (2004) 691–699.
[27] Project Daedalus Study Group: A. Bond, et al., Project Daedalus – the final Report on the BIS starship study, JBIS Interstellar Studies, Supplement (1978) 13–20.
[28] James Webb Space Telescope User Documentation, (13 April 2018), pp. 763–764 https://jwst-docs.stsci.edu.
[29] P. Lubin, A Roadmap to interstellar flight, J. Br. Interplanet. Soc. (JBIS) 69 (2016) S1–S192.
[30] N. Perakis, J. Gutsmiedl, A. Koop, M.J. Losekamm, N. Perakis, L. Schrenk, Project Dragonfly: A Feasibility Study of Interstellar Travel Using Laser-Powered Light Sail Propulsion, (2016) To be submitted to acta Astronautica.
[31] A.M. Hein, K.F. Long, D. Fries, N. Perakis, A. Genovese, S. Zeidler, M. Langer, R. Osborne, R. Swinney, J. Davies, B. Cress, M. Casson, A. Mann, R. Armstrong, The Andromeda Study: A Femto-spacecraft mission to Alpha Centauri, (2017).
[32] R. Heller, M. Hippke, Deceleration of high-velocity interstellar photon sails into bound orbits at α Centauri, Astrophys. J. Lett. 835 (2017) L32.
[33] R. Forward, Roundtrip interstellar travel using laser-pushed lightsails, J. Spacecraft Rockets 21 (1984) 187–195.
[34] https://i4is.org/project-dragonfly-competition-workshop/.